Forced to Align: Flow-Induced Long-Range Alignment of Hierarchical Molecular Assemblies from 2D to 3D

Shern-Long Lee,[†] Zhongyi Yuan,[‡] Long Chen,[‡] Kunal S. Mali,[†]* Klaus Müllen[‡]* and Steven De Feyter[†]*

[†]KU Leuven-University of Leuven, Department of Chemistry, Division of Molecular Imaging and Photonics Celestijnenlaan 200F, B-3001 Leuven, Belgium, [‡]Max Planck Institute for Polymer Research, D-55128 Mainz, Germany

Supporting Information Placeholder

ABSTRACT: Nanostructured molecular thin films adsorbed on solid surfaces form the basis of numerous applications. Long-range order within adsorbed molecules is very often a desirable property for such systems. In this contribution, we report a simple and efficient method to fabricate well-aligned thin films of organic molecules over a few millimeter squares. The strategy involves use of capillary force in a two-step flow method to induce large-area alignment of multilayers of molecules at the organic liquid-solid interface. Furthermore, we also demonstrate the influence of alignment on the electron transport through these well–aligned thin films using scanning tunneling spectroscopy.

Development of robust strategies for the fabrication of large-area, defect-free nanostructured surfaces is a major challenge in advanced surface engineering.[1] Such surfaces are important as templates or as functional elements in applications including crystal growth, catalysis, sensing and organic electronic devices.[2,3] Lithographic techniques have been extensively used to engineer ordered surface nanostructures, but they are rapidly reaching processing and scaling limits.[4] Molecular self-assembly has been recognized as a promising alternative for controlled bottom-up fabrication of functional surfaces with tailor-made properties.[5,6] This approach enables the high-precision construction of well-ordered nanostructures on solid surfaces using organic molecules as building blocks.[7-9] Furthermore, solution processing of organic thin films, where molecules self-assemble at the liquid-solid interface, has proven to be a beneficial deposition technique due to its facile, versatile and cost-effective nature.[10]

The self-assembly approach however, often suffers from limitations imposed by 2D polymorphism[11], limited domain sizes and lack of orientation control of domains. These factors contribute to the undesirable polycrystallinity of the thin films. This especially becomes a serious issue for organic thin film devices comprising π-conjugated molecules where the relative orientation of molecules within and in-between layers is crucial to enable efficient charge transport across electrodes. In fact, the influence of grain boundary orientation on the performance of organic field effect transistors (OFETs) has been recently demonstrated where large, well-oriented grains have been shown to increase the charge carrier mobility by several orders of magnitude.[12]

Given that long-range order is likely the most desired parameter for numerous applications, many efforts have been devoted to the development of alignment techniques.[13] A series of solution-based methods such as dip coating,[14] zone casting,[15] dewetting[16] and solution shearing[17] have evolved over the past decade. Liquid flow has been shown to align a variety of materials such as liquid crystals,[18] polymers,[19] metal nanorods,[20] organic nanofibers[21] and nanoparticles[22] on solid surfaces. Despite these efforts, forcing well-aligned organization of molecules within multilayered nanostructured thin films over large length scales remains a challenge.

Here we demonstrate a facile two-step flow method (Scheme 1) to produce well-ordered thin films of a rigid polyaromatic hydrocarbon (PAH), hexarylene diimide[23] (HDI, Figure 1a), at the liquid-solid interface. In our simple technique,[17] the solution flow is produced *via* capillary force generated by simply contacting a clean tissue paper to the substrate immediately after drop casting the solution on surface. Scanning tunneling microscopy (STM) reveals that the polycrystallinity of the films obtained upon simple drop casting could be significantly reduced using the first flow (*flow I*) which yields up to 5×5 mm^2 domains of uniaxially assembled HDI network. Application of a second flow (*flow II*) to this surface generates well-aligned multilayers which exhibit excellent collinear packing of molecules within different layers.

The two-step flow method enables reproducible and reliable fabrication of large-area, well-aligned multilayers which are not formed spontaneously upon deposition from solution. Furthermore, this well-aligned superstructure allows for more efficient electron transport *via* the π-stacking of the conjugated molecules as revealed by scanning tunneling spectroscopy (STS). The application of flow for the alignment of surface adsorbed small molecules as described here is virtually unexplored for monolayers[17] and unprecedented for multilayers. The simplicity of this method renders it a promising yet cost-effective approach for the long-range alignment of molecular thin films.

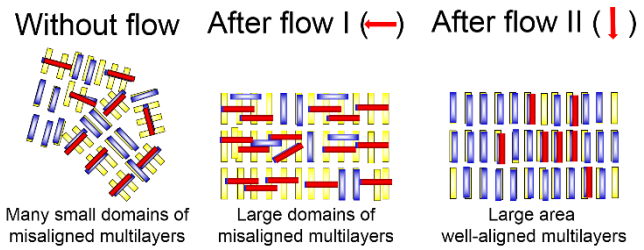

SCHEME 1. Two-step flow method for the fabrication of long-range ordered hierarchical thin films. The rectangles with different colors represent molecules adsorbed in different layers. Red arrows indicate flow direction.

HDI belongs to the family of rylene diimide chromophores which consist of naphthalene units linked in the *peri*-position.[24] It is a rigid PAH with relatively large aspect ratio (4.2, excluding the alkyl substituents). The anisotropic shape of this molecule makes it an ideal choice for flow-induced assembly since a number of 1D nanostructures have been efficiently aligned using such methods.[13] Furthermore, due to strong π-stacking interactions, HDI exhibits a pronounced aggregation tendency both in solution and on the surface. The multilayers of HDI are stable and up to three layers could be obtained at the 1, 2, 4-trichlorobenzene (TCB)/highly oriented pyrolytic graphite (HOPG) interface.[23] The rylene dyes are excellent colorants, good electron-acceptors and possess exceptional chemical and photochemical stability. Functionalized rylene derivatives have garnered significant attention in optoelectronic applications, dye chemistry and supramolecular chemistry.[24]

Figure 1b and 1c show typical STM images of the HDI assemblies obtained without and with the flow treatment at the TCB/HOPG interface, respectively. The spontaneously self-assembled structure (without flow) typically shows multiple small domains (average domain size ~ 60 × 60 nm²) oriented at angles determined by the graphite lattice vectors (Figure S1-Supporting Information). The rod-like features evident in the STM images correspond to the aromatic backbones of the HDI molecules. The alkyl chains are located in the dark troughs in between the molecular rows and could not be resolved. The variation in the apparent height of the rod-like features arises from molecules adsorbed in different layers.[23] Thus, both the less bright and bright features correspond to the rylene units adsorbed in layers closer to and away from the surface, respectively.

The rylene units adsorbed in the lower layer are arranged in rows and their long axes run nearly perpendicular to the row axis. The features with the highest apparent height are often aligned at an angle with respect to the molecules in the lower layer (Figure 1b). The histogram in Figure 1e shows the angle distribution of molecules adsorbed in the upper layers with respect to those in lower layers. The population is centered around three angles: a majority population oriented at +/- 70° with respect to lower molecules and a well-aligned (0°) minority population.

The polycrystalline morphology of the surface can be significantly changed by application of the first flow instantaneously after the deposition of the solution droplet onto the HOPG surface. This is achieved by contacting a tissue paper

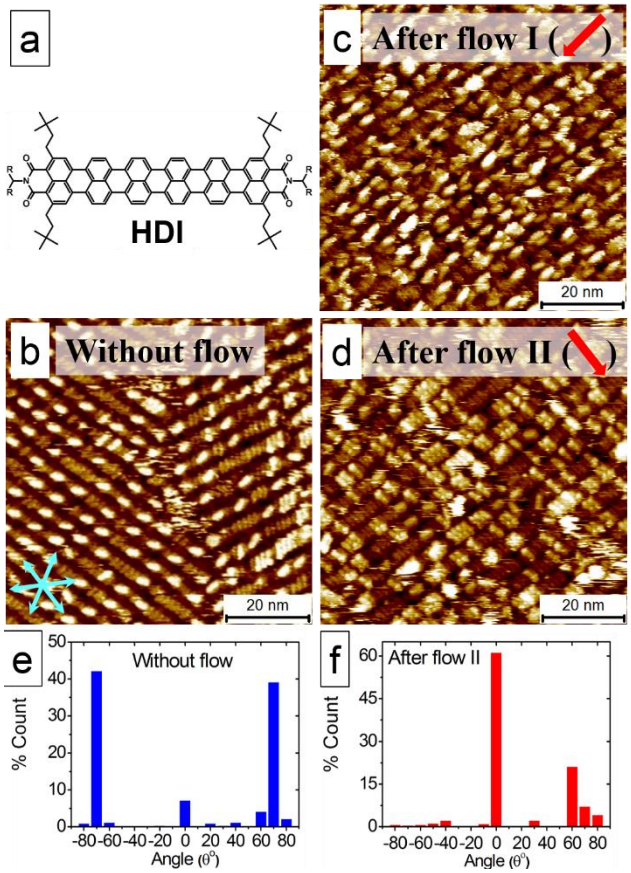

FIGURE 1. (a) Molecular structure of HDI (R = $-C_{11}H_{23}$). (b) STM image showing multidomain morphology of the HDI thin film spontaneously formed at the TCB/HOPG interface (C_{HDI} = 1.7 × 10⁻⁵ M). Cyan arrows indicate graphite symmetry axes. (c) STM image illustrating change in the morphology as a result of *flow I* which causes formation of large domains extending up to several mm². *Flow II* is applied to this surface in an orthogonal direction to the first flow. Red arrows in (c) and (d) indicate the two flow directions. (d) Final result of the two-step flow process that yields highly aligned large-area multilayers. Panels (e) and (f) show histograms of angle distribution for molecules adsorbed in upper layers with those in the lower layers before and after the flow treatment. Angle 0° in the histograms refers to the well-aligned population. (Imaging conditions: V_{bias} = 750 mV, I_{set} = 100 pA).

(Kimwipe) to a freshly deposited droplet such that the flow is generated along the normal to one of the graphite symmetry axes. The generated flow field is expected to be a combination of a confined shear flow with extensional components. STM analysis of the surface after *flow I* shows essentially the same packing however, the flow induces formation of large domains containing uniaxially aligned lower layers that extend over several square millimeters (Figure S3). The increase in the domain area achieved is almost ten orders of magnitude. It must be noted that the efficiency of the first flow is excellent only up to 5 mm from the contact line. In other words, *flow I* produces up to 5 × 5 mm² uniaxial domains. The multidomain mosaics are observed in the regions out of this active zone. Secondly, the molecules adsorbed in the upper layers (features with highest apparent height in Figure 1c), remain randomly

oriented with respect to the lower layers. The angle distribution of these upper layer molecules remains identical to that observed before the application of the first flow (Figures S1 and S3).

The orientation of the HDI molecules in the upper layers can be affected by a subsequent flow applied nearly parallel to the long axis of the HDI molecules adsorbed in lower layers which also coincides with one of the main symmetry axes of the graphite lattice. *Flow II* forces the molecules in the upper layers to align parallel to those adsorbed in the lower layers (Figure 1d). The angle distribution is significantly affected by the second flow thus aligning a majority of the population as shown in the histogram provided in Figure 1f. Thus, the two-step flow method produces well-defined collinear multilayers of HDI on HOPG over large areas (Figure S4). Furthermore, the alignment process can be monitored *in situ* by obtaining sequential STM images while *flow II* is being applied to the sample. These images show gradual change in the orientation of the molecules in subsequent scans (Figure S13). The efficiency of *flow II* is maximum up to 2.5 mm from the second contact line after which misaligned molecules in the upper layers are observed. The well-aligned molecular layers fabricated using the aforementioned method remain stable and do not undergo significant reorganization for several days when stored under ambient conditions or upon heating to 100°C (Figure S6 and S7).

To evaluate the total number of complete layers, the aligned surface was rinsed gently with TCB. STM images obtained on the rinsed surface revealed a relatively uniform, striped pattern. Figure 2a shows that this motif is a bilayer with a small fraction of HDI molecules adsorbed on top of it. Generation of defects using voltage pulses applied to the STM tip enabled visualization of the bare graphite surface underneath thus allowing a correct determination of the number of layers (Figure S8). This exercise confirmed that the structural motif templating the upper layers is indeed a bilayer. The detailed structure of the bilayer along with a molecular model is provided in Figure 2b and 2c, respectively.

The efficiency of the flow process is also dependent on a number of extrinsic variables. An overview of a large number of STM images indicates that the step edges present on the HOPG substrate act as obstacles to the flow. Small domains of non-aligned molecules are often observed near step edges. These regions nevertheless, are fairly small (~ 5%) compared to the overall aligned area (Figure S10). The direction of the flow with respect to the symmetry axes of the HOPG lattice is also critical to the process.[17] STM images obtained on spontaneously self-assembled HDI assemblies reveal that molecular rows are oriented nearly (+/-11°) along the normal to the HOPG symmetry axes. Given the propensity of row formation along these directions, *flow I* was always applied along these reference directions. A control experiment where *flow I* was applied along the main symmetry directions of the HOPG lattice turned out to be relatively inefficient with the surface exhibiting polycrystalline morphology (Figure S11).

Although liquid flows have been used extensively to align rod-shaped particles, the present results are striking in view of the extremely small length scales involved. It is well-known that shear flow can cause particles to tumble due to vorticity. The tumbling of individual particles enables the

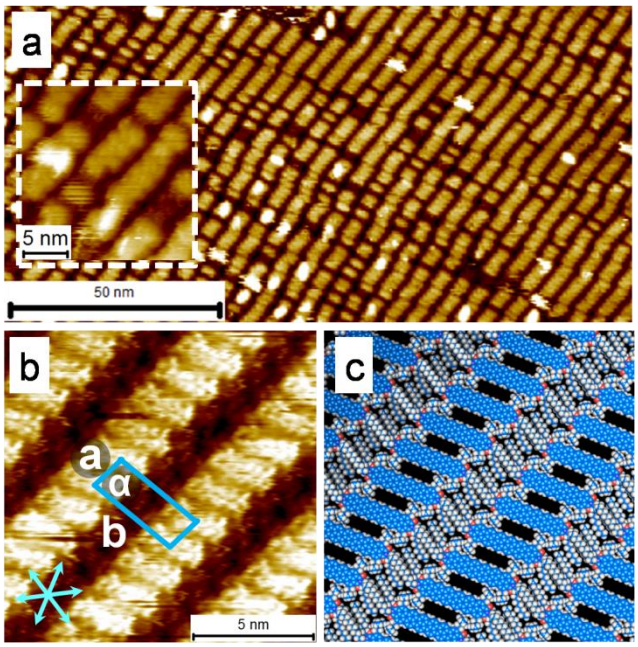

FIGURE 2. (a) Large-scale STM image showing the stable bilayer structure obtained after rinsing the flow-aligned molecular layers. The inset shows a magnified area. (b) STM image showing the arrangement of the HDI molecules in the bilayer. Unit cell parameters a = 1.47 ± 0.11 nm, b = 4.35 ± 0.08 nm, α = 87.3 ± 1.4°. (c) Corresponding molecular model Imaging conditions: V_{bias} = 750 mV, I_{set} = 100 pA.

long-range alignment when considered in a time averaged sense. For the flow generated by the capillary suction, an extensional component[25] will enhance the alignment. However, for this process to be efficient, advection (movement of the particles *via* the bulk flow of the liquid) should dominate diffusion. The extremely small length scales involved here necessitate strong flow conditions for increased advection. We believe that the highly confined nature of the applied shear flow in combination with the extensional components in the flow field generate the high-flow rates mandatory for efficient alignment.

Besides the aforementioned factors intrinsic to the flow, one has to also take into consideration the importance of molecule-substrate and intermolecular interactions. As mentioned before, the specific epitaxial relationship between molecular rows and the substrate lattice compels the application of the flow only along certain symmetry directions.[17] Such a directional flow creates a dynamic environment in which the mobility of molecules at the interface is enhanced. This enables efficient mass transport across the interface in a kinetically driven process - a prerequisite for large-area patterning[21] at the liquid-solid interface. *Flow II* then helps the molecules to reach the optimal orientation with respect to the lower layers as it is readily expected that the collinear packing is favored due to better π-stacking interactions.

STS carried out on the flow aligned films revealed that the three-layered structure of HDI has a remarkably reduced band gap (*ca.* 0.2 eV) compared to that of the first layer of HDI adsorbed on HOPG (Figure 3b) or the misaligned

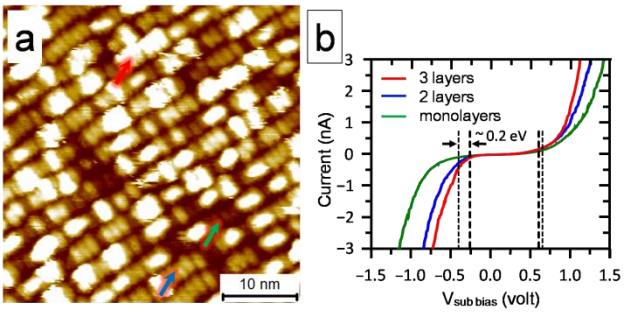

FIGURE 3. (a) Surface prepared by a two-step flow. The green, blue and red arrows depict 1-, 2-, and 3-layers. (b) Tunneling spectra obtained over the positions of 1-, 2-, and 3-layers of HDI. Each I-V curve was averaged from 72, 69, and 64 curves for 1-, 2-, and 3-layered structures of HDI, respectively. Parameters for STS measurements: V_{bias} = 750 mV, I_{set} = 100 pA.

structure of HDI (Figure S14). Figure 3 shows a surface prepared by the two-step flow method along with the spectroscopic data.

The reduced band gap can be ascribed to the effect of the energy-level coupling in the π-stacked layer of HDI. Such phenomena have been explained in the past using the *Davydov splitting model*.[26] It has been pointed out that, for closely spaced molecules in a π-stack, the HOMO and LUMO levels of the isolated molecule split and delocalize over the whole π-stacked complex, giving rise to new molecular states with reduced HOMO-LUMO gap.[27] The appreciable tunneling current for the layered packing of HDI also suggests the existence of strong vertical π-π interactions which enable efficient 'through-space'[28] electron transport within the HDI superstructures.

In conclusion, we have demonstrated a simple yet efficient solution-based strategy to obtain large-area, well-aligned thin films of organic molecules on a solid surface. The two-step flow process efficiently reduces the polycrystallinity of the thin films and also helps to align misoriented molecules. The effect of multilayer formation and alignment is reflected in the electron transport within these layers as probed by STS. This study unveils important aspects of flow-induced molecular assembly on a surface and demonstrates how such a flow can tune material features such as electron transport *via* control over molecular organization. The present approach can be employed for large-area alignment within multilayered thin films that comprise rigid polyaromatic molecules with relatively large aspect ratios.

Supporting Information

Experimental methods and additional STM and STS data. This material is available free of charge *via* the Internet at http://pubs.acs.org.

AUTHOR INFORMATION

Corresponding Author

Kunal.Mali@chem.kuleuven.be; muellen@mpip-mainz.mpg.de; Stven.DeFeyter@chem.kuleuven.be

Notes

The authors declare no competing financial interests.

ACKNOWLEDGMENT

This work is supported by the Fund of Scientific Research–Flanders (FWO), KU Leuven (GOA 11/003), Belgian Federal Science Policy Office (IAP-7/05), and DFG Priority Program SPP 1355, SENSOR. S.-L. L. is FWO Pegasus Marie Curie Fellow. The research leading to these results has also received funding from the European Research Council under the European Union's Seventh Framework Programme (FP7/2007-2013)/ERC Grant Agreement no. 340324. We thank Prof. J. Vermant for comments on the manuscript.

REFERENCES

(1) Gates, B. D.; Xu, Q.; Stewart, M.; Ryan, D.; Willson, C. G.; Whitesides, G. M. *Chem. Rev.* **2005**, *105*, 1171.
(2) Arias, A. C.; MacKenzie, J. D.; McCulloch, I.; Rivnay, J.; Salleo, A. *Chem. Rev.* **2010**, *110*, 3.
(3) De Luca, G.; Pisula, W.; Credgington, D.; Treossi, E.; Fenwick, O.; Lazzerini, G. M.; Dabirian, R.; Orgiu, E.; Liscio, A.; Palermo, V.; Müllen, K.; Cacialli, F.; Samorì, P. *Adv. Funct. Mater.* **2011**, *21*, 1279.
(4) Ito, T.; Okazaki, S. *Nature* **2000**, *406*, 1027.
(5) Tait, S. L. *ACS Nano* **2008**, *2*, 617.
(6) Ciesielski, A.; Palma, C. A.; Bonini, M.; Samori, P. *Adv. Mater.* **2010**, *22*, 3506.
(7) Yang, Y.; Wang, C. *Chem. Soc. Rev.* **2009**, *38*, 2576.
(8) Xue, Y.; Zimmt, M. B. *J. Am. Chem. Soc.* **2012**, *134*, 4513.
(9) Li, S.-S.; Northrop, B. H.; Yuan, Q.-H.; Wan, L.-J.; Stang, P. J. *Acc. Chem. Res.* **2009**, *42*, 249
(10) Han, W.; Lin, Z. *Angew. Chem. Int. Ed.* **2012**, *51*, 1534.
(11) Ahn, S.; Matzger, A. J. *J. Am. Chem. Soc.* **2010**, *132*, 11364.
(12) Rivnay, J.; Jimison, L. H.; Northrup, J. E.; Toney, M. F.; Noriega, R.; Lu, S.; Marks, T. J.; Facchetti, A.; Salleo, A. *Nat. Mater.* **2009**, *8*, 952.
(13) Su, B.; Wu, Y.; Jiang, L. *Chem. Soc. Rev.* **2012**, *41*, 7832.
(14) Huang, J.; Fan, R.; Connor, S.; Yang, P. *Angew. Chem. Int. Ed.* **2007**, *46*, 2414.
(15) Pisula, W.; Menon, A.; Stepputat, M.; Lieberwirth, I.; Kolb, U.; Tracz, A.; Sirringhaus, H.; Pakula, T.; Müllen, K. *Adv. Mater.* **2005**, *17*, 684.
(16) van Hameren, R.; Schon, P.; van Buul, A. M.; Hoogboom, J.; Lazarenko, S. V.; Gerritsen, J. W.; Engelkamp, H.; Christianen, P. C.; Heus, H. A.; Maan, J. C.; Rasing, T.; Speller, S.; Rowan, A. E.; Elemans, J. A.; Nolte, R. J. *Science* **2006**, *314*, 1433.
(17) Lee, S.-L.; Chi, C.-Y. J.; Huang, M.-J.; Chen, C.-h.; Li, C.-W.; Pati, K.; Liu, R.-S. *J. Am. Chem. Soc.* **2008**, *130*, 10454.
(18) Yoshio, M.; Mukai, T.; Ohno, H.; Kato, T. *J. Am. Chem. Soc.* **2004**, *126*, 994.
(19) Lee, S.-L.; Lin, N.-T.; Liao, W.-C.; Chen, C.-h.; Yang, H.-C.; Luh, T.-Y. *Chem.-A Eur. J.* **2009**, *15*, 11594.
(20) Kim, J.; Peretti, J.; Lahlil, K.; Boilot, J. P.; Gacoin, T. *Adv. Mater.* **2013**, *25*, 3295.
(21) Raez, J.; Moralez, J. G.; Fenniri, H. *J. Am. Chem. Soc.* **2004**, *126*, 16298.
(22) Grzelczak, M.; Vermant, J.; Furst, E. M.; Liz-Marzán, L. M. *ACS Nano* **2010**, *4*, 3591.
(23) Yuan, Z.; Lee, S.-L.; Chen, L.; Li, C.; Mali, K. S.; De Feyter, S.; Müllen, K. *Chem.- A Eur. J.* **2013**, *19*, 11842.
(24) Weil, T.; Vosch, T.; Hofkens, J.; Peneva, K.; Mullen, K. *Angew. Chem. Int. Ed.* **2010**, *49*, 9068.
(25) Schroeder, C. M.; Babcock, H. P.; Shaqfeh, E. S. G.; Chu, S. *Science* **2003**, *301*, 1515.
(26) Cornil, J.; Beljonne, D.; Calbert, J. P.; Bredas, J. L. *Adv. Mater.* **2001**, *13*, 1053.
(27) Gesquière, A.; De Feyter, S.; Schoonbeek, F.; van Esch, J.; Kellogg, R. M.; Feringa, B. L. *Nano Lett.* **2001**, *1*, 201.

(28) Batra, A.; Kladnik, G.; Vazquez, H.; Meisner, J. S.; Floreano, L.; Nuckolls, C.; Cvetko, D.; Morgante, A.; Venkataraman, L. *Nat. Commun.* **2012**, *3*, 1086.

Table of Contents